IEEE Access
Multidisciplinary : Rapid Review : Open Access Journal

Received 29 January 2024, accepted 25 February 2024, date of publication 4 March 2024, date of current version 11 March 2024.

Digital Object Identifier 10.1109/ACCESS.2024.3373611

RESEARCH ARTICLE

Practical Circuit-Based Design Approach for Waveguide Lowpass Filter With Extremely Steep Skirt Response

SANGGU LEE[1], JONGHEUN LEE[2], (Graduate Student Member, IEEE), DUCKKI BAEK[3], PILYONG LEE[3], AND JUSEOP LEE[2], (Senior Member, IEEE)

[1]LIGNex1, Yongin-si, Gyeonggi-do 16911, South Korea
[2]Department of Computer and Radio Communications Engineering, Korea University, Seoul 02841, South Korea
[3]PILAS, Yongin-si, Gyeonggi-do 16914, South Korea

Corresponding author: Juseop Lee (juseoplee@gmail.com)

This work was supported by the National Research Foundation of Korea (NRF) under Grant NRF-2022R1A2B5B01001340.

ABSTRACT This paper presents a practical circuit-based design approach for a waveguide lowpass filter with a steep skirt response. For efficient filter design, the proposed structure employs a cascade of troughs with the same physical dimensions. Having identical troughs in most parts of a filter structure greatly alleviates the design difficulty. In addition, our filter design approach is largely based on circuit analysis rather than electromagnetic simulations, greatly expediting filter designs. A WR-75 waveguide lowpass filter example has been designed, fabricated, and measured for demonstration.

INDEX TERMS Circuit, lowpass, trough, waveguide, WR-75.

I. INTRODUCTION

Lowpass filters are widely used in wireless systems, for example, to suppress harmonics and separate transmitting and receiving signals [1], [2], [3], [4], [5]. More specifically, lowpass filters of waveguide structures are commonly used where low-loss performance is required. A classical waveguide lowpass filter structure can be found in [6] and [7], and comprehensive research on various waveguide lowpass structures such as corrugated waveguide filters [8], [9], [10], [11], [12], [13], [14], [15], [16], [17], [18], ridged waveguide filters [19], [20], [21], [22], [23], [24], [25], waffle-iron waveguide filters [26], [27], [28], [29], [30], [31], [32] has been carried out. In addition, new design techniques based on a windowed quasi-periodic structure [33], [34], [35], [36], elliptic posts prototype [37], and meandered topology [38] have been presented.

In general, lowpass waveguide filters have evolved in such a way as to have more complex structures, which makes the design approaches rely more on electromagnetic simulations. However, full-wave simulations do not allow us to instantly predict the change of the response shape when one or multiple physical dimensions change. This makes a filter design take a substantial amount of time.

Hence, this paper presents a practical design method for a corrugated waveguide lowpass filter. Unlike most corrugated

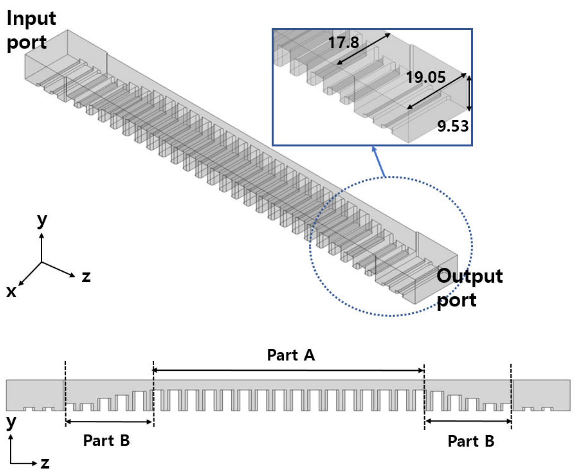

FIGURE 1. Perspective and cross-sectional views of the entire filter structure.

The associate editor coordinating the review of this manuscript and approving it for publication was Photos Vryonides.

waveguide lowpass filters available in the literature, this work deals with a filter structure with corrugations on one side of it. Incorporating corrugations on one side instead of two sides greatly reduces the fabrication time and the structure's height to their halves approximately. This paper will also describe another benefit of a single-sided corrugated waveguide filter from the perspective of fabrication difficulty.

Our design approach can be differentiated from the conventional approaches in that the main part of the filter structure is a simple cascade of identical troughs. To the best of our knowledge, this greatly reduces the degree of design difficulty, which has not been demonstrated to date. In addition, our approach mainly employs circuit analysis rather than time-consuming electromagnetic simulations.To verify the circuit-based design approach, the design of a WR-75 waveguide lowpass filter will be demonstrated in this paper. This paper also includes a comparison of the steepness of the skirt response between our lowpass filter structure and those available in the literature. This highlights that the presented design method can handle a tough specification for a skirt steepness.

II. FILTER DESIGN

The target specifications of our filter design are given as follows

- Input and output ports: WR-75 waveguide
- Return loss: $\geq$ 15 dB in the passband (10.5 - 12.5 GHz)
- Attenuation $\geq$ 90 dB in the stopband (12.75 - 15.0 GHz)

According to the specifications, there is a very narrow transition band between the passband and the stopband. It is worth highlighting that attenuation is required to increase by 90 dB within the 0.25 GHz transition band. To evaluate the steepness of the skirt response in a quantitative manner, a figure of merit (FOM) is defined and proposed as follows:

$$\text{FOM}_{A\text{ dB}} = \frac{f_3 - f_2}{f_2 - f_1} \tag{1}$$

where f_1 and f_2 are the start and stop frequencies of the passband, respectively, and f_3 is the frequency at which a certain amount of attenuation (A dB) begins to be observed. In the target specifications above, f_1 and f_2 are 10.5 GHz and 12.5 GHz, respectively, and f_3 is 12.75 GHz with A= 90. Hence, our filter design is required to have $\text{FOM}_{90\text{ dB}}$ of 0.125. According to (1), a smaller FOM indicates a steeper skirt response. The FOM in (1) can be interpreted as the transition band's width normalized to the passband's width. The reason for normalization is that having a wider passband (f_2-f_1) makes it more challenging to achieve a specified attenuation in the given absolute transition band.

A lowpass filter can satisfy the above specifications because there is no attenuation requirement below the passband. Extensive work on lowpass corrugated waveguide filters has been reported to date [6], [7], [8], [9], [10], [11], [12], [13], [14], [15], [16], [17], [18]. However, the designs of the waveguide structures demonstrated by earlier works are considered sophisticated, as neighboring troughs have different dimensions from each other. More specifically, a trough's dimensions differ from its neighbor's. As the number of dimensions of a filter structure that need to be determined increases, it takes longer to design, especially when the design relies highly on electromagnetic simulations. Hence, we propose a corrugated waveguide filter structure mainly composed of identical troughs, and its efficient design method mostly avoids electromagnetic simulations.

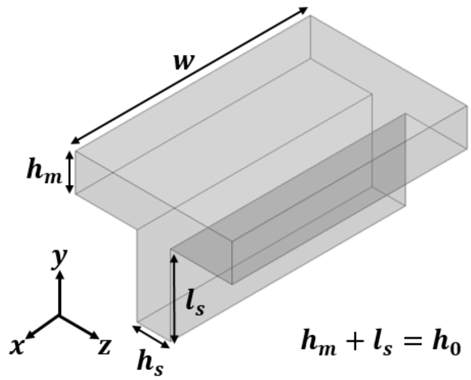

(a)

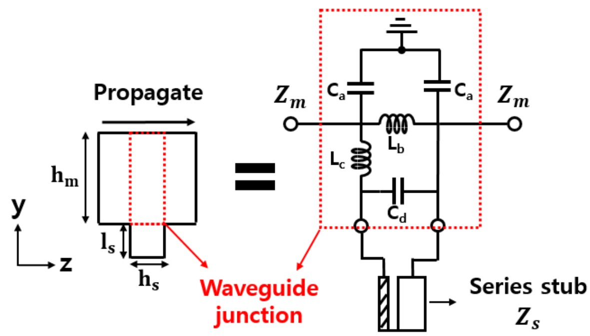

(b)

FIGURE 2. (a) Single trough structure. (b) equivalent circuit.

Fig. 1 shows the entire structure of our filter. It is mainly composed of parts A and B. Part A has identical troughs cascaded by a uniform reduced-height waveguide. Part B consists of troughs with different dimensions in the y direction. For simplicity, the dimension measured from the bottom of each trough to the top surface of the waveguide structure remains constant and equals the height of WR-75. The input and output ports are WR-75 according to the specification. Parts A and B are narrower than WR-75 by a small amount, and the reason will be discussed later.

A. PART A

Fig. 2(a) shows the single trough comprising part A shown in Fig. 1. It is connected to the reduced-height uniform waveguide. The trough and the uniform waveguide have the same width denoted by w. The heights of the trough and the uniform waveguide are denoted by h_s and h_m, respectively, and the length of the trough is l_s.

The structure shown in Fig. 2(a) can be modeled as shown in Fig. 2(b). It is shown that the trough connected to the E-plane of the main waveguide is equivalent to the short-circuited series stub. In addition, the waveguide junction is characterized by several lumped elements whose susceptance values are given by [39]

$$B_a = \frac{\pi h_s}{Z_m \lambda_g} \cdot \left[1 - \frac{h_s}{2\pi h_m} + \frac{8}{\pi^2}\left(\frac{2h_s}{\lambda_g}\right)^2 (1 - 0.368\frac{h_s}{h_m})\right]$$
$$B_b = 1.1\frac{h_s}{Z_m \lambda_g} \cdot \left[1 - 0.227\frac{h_s}{h_m} + 0.008\left(\frac{h_s}{h_m}\right)^2\right]$$
$$B_c = \frac{\lambda_g}{2 Z_m \pi h_s}$$
$$B_d = \frac{h_m}{Z_m \lambda_g} \cdot \left[2ln\left(\frac{e h_m}{2h_s}\right) + 1.1\left(\frac{h_s}{h_m}\right) - 0.167 \cdot \left(\frac{h_s}{h_m}\right)^2 + 0.008\left(\frac{h_s}{h_m}\right)^3\right] \quad (2)$$

where

$$C_a = \frac{B_a}{2\pi f}$$
$$L_b = \frac{1}{2\pi f \cdot B_b}$$
$$L_c = \frac{1}{2\pi f \cdot B_c}$$
$$C_d = \frac{B_d}{2\pi f} \quad (3)$$

As the equivalent circuit parameters in (2) are given in terms of the physical dimensions, we can instantly obtain the frequency response of the waveguide structure shown in Fig. 2(a) when the dimensions are provided. Hence, we can rapidly analyze the impact of the physical dimensions of the single trough (l_s, w, and h_s) on the frequency response without electromagnetic simulations. In our design, we have set the trough's initial width (w) to that of the standard WR-75 waveguide. The height of the trough (h_s) was initially determined to be 2.5 mm, considering the fabrication by milling. Fig. 3(a) shows the variation of the transmission response of the single trough circuit (Fig. 2(b)) with respect to the length of the trough, l_s. Both the results of electromagnetic simulations of the single trough structure and the responses of the equivalent circuit are shown in Fig. 3(a), and it can be concluded that a filter design can be carried out relying on the equivalent circuit rather than electromagnetic simulations since there is a good agreement between the responses of the equivalent circuit and the results of the electromagnetic simulations. The small discrepancies can be attributed to the existence of an inherent inaccuracy in modeling a physical structure by an equivalent circuit or in subdividing a structure into finite elements for an electromagnetic simulation or both. It is obvious that the transmission zero moves to a lower frequency when the length of the trough modeled by the series stub increases. In consideration of the specifications, the length of trough has been set to 6.5 mm.

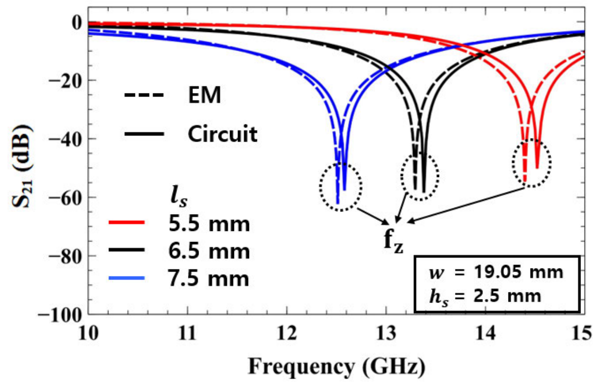

l_s	$f_{Z_{EM}}$	$f_{Z_{Cir}}$	Accuracy
5.5 mm	14.39 GHz	14.52 GHz	99.1 %
6.5 mm	13.29 GHz	13.38 GHz	99.33 %
7.5 mm	12.51 GHz	12.58 GHz	99.44 %

(a)

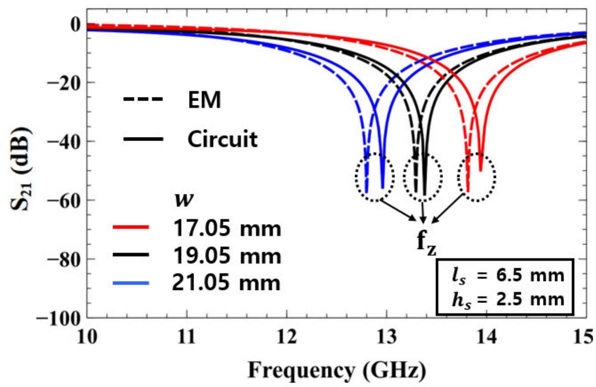

w	$f_{Z_{EM}}$	$f_{Z_{Cir}}$	Accuracy
17.05 mm	13.81 GHz	13.94 GHz	99.07 %
19.05 mm	13.29 GHz	13.38 GHz	99.33 %
21.05 mm	12.8 GHz	12.96 GHz	98.77 %

(b)

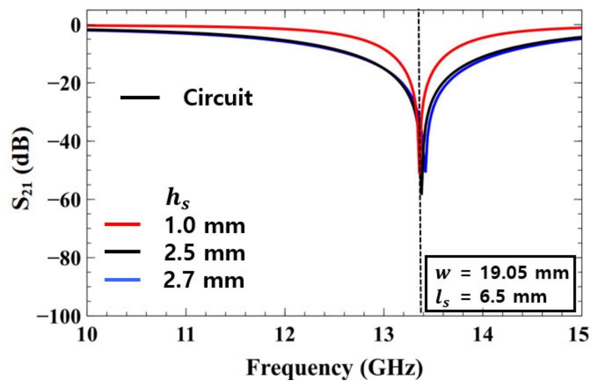

(c)

FIGURE 3. Variations of the transmission response of the circuit in Fig. 2(b) with respect to (a) l_s, (b) w, and (c) h_s. (solid lines: circuit, dashed lines: em).

Fig. 3(b) shows the transmission response with the variation of w. It can be observed that increasing w makes the transmission zero move to a lower frequency. Considering the input and output ports for our target filter specification, we have initially set w to WR-75 for simplicity.

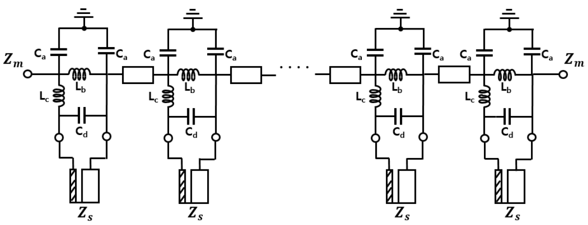

FIGURE 4. The circuit schematic of part A with multiple troughs.

The last physical parameter we have to consider is h_s and Fig. 3(c) shows the transmission responses with various trough heights. The plots in Fig. 3(c) are obtained from the equivalent circuit, and the results of electromagnetic simulations are not included in this figure for the sake of readability. It can be seen that h_s has little impact on the location of the transmission zero but a smaller h_s is preferred from the point of view of the skirt response. In addition, h_s larger than 2.5 mm makes little difference in the response but the filter size increases with h_s. According to the aforementioned discussions, the initial value 2.5 mm can be used in our filter design, but it has been adjusted to 2.7 mm in order to give more room to a milling bit. Having two troughs, one on each E-plane of a waveguide, is equivalent to having a single trough on one side with a larger h_s. Hence, a single-sided corrugated waveguide filter is more favorable than a double-sided one in terms of milling.

Using the initial dimensions of the trough and the uniform waveguide, we can design part A by cascading the troughs identical to one another. In this step, our design utilizes the equivalent circuit for the single trough. Fig. 4 shows the circuit schematic of part A with multiple troughs. Each transmission line represents a reduced-height waveguide, namely main waveguide, between two troughs. Its length (spacing between troughs) is set to 2.7 mm which is the same as h_s since a small spacing widens the overall stopband and reduces the insertion loss as well as the overall filter length [11]. Fig. 5 shows the variation of the transmission response of the circuit shown in Fig. 4 with respect to the number of the troughs. It can be clearly observed that the skirt response becomes steeper as the number of the troughs increases. It can also be observed that cascading identical troughs produces repeated transmission zeros at the same frequency leading to an extremely steep skirt response. In consideration of the attenuation specification, it can be concluded that 15 troughs are sufficient for the required steepness (90 dB/0.25 GHz) of the skirt response

B. PART B

Part A described in the previous section (section II-A) does not provide a good return loss performance. This issue can be addressed by adding part B to both sides (input and output) of part A. Part B is similar to part A but the difference lies in the fact that the height of the troughs gradually changes. Hence, each trough is connected to the non-uniform waveguide whose height changes as shown in

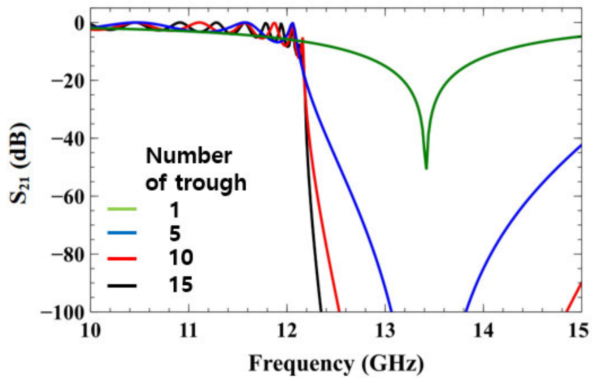

FIGURE 5. Variation of the transmission response of the circuit in Fig. 4 with respect to the number of troughs. (w= 19.05, l_s= 6.5, h_s= 2.7). (All units in mm)

Fig. 6(a). In other words, the main waveguide in part B is a step-impedance waveguide. In our filter design, the structure shown in Fig. 6(a) has been considered to have five components: trough, waveguides with heights, h_{mn} and h_{mn+1} ($h_{mn} < h_{mn+1}$), waveguide junction with height h_{mn}, and waveguide step for height change between h_{mn} and h_{mn+1}. Hence, the single trough connected to the step-impedance waveguide shown in Fig. 6(a) can be modeled as shown in Fig. 6(b). It is shown that the transmission lines with different impedances (z_{mn} and z_{mn+1}) represent the step-impedance waveguide. The lumped elements excluding the capacitor with susceptance B_{n+1} are for modeling the waveguide junction with height h_{mn}, and their values are given in (2) and (3). The capacitor with susceptance B_{n+1} represents the waveguide step (increase of the waveguide height), and B_{n+1} is given by [39]

$$B_{n+1} = \frac{4h_{mn+1}}{Z_{mn+1}\cdot\lambda_g}\cdot\Bigg[2\frac{A_{n+1}+A'_{n+1}+2C_{n+1}}{A_{n+1}\cdot A'_{n+1}-C^2_{n+1}} + ln\left(\frac{1-\alpha^2_{n+1}}{4\alpha_{n+1}}\right)\left(\frac{1+\alpha_{n+1}}{1-\alpha_{n+1}}\right)^{\frac{\alpha_{n+1}+\frac{1}{\alpha_{n+1}}}{2}} + \left(\frac{h_{mn+1}}{2\lambda_g}\right)^2\left(\frac{1-\alpha_{n+1}}{1+\alpha_{n+1}}\right)^{4\alpha_{n+1}} \cdot\left(\frac{5\alpha^2_{n+1}-1}{1-\alpha^2_{n+1}}+\frac{4\alpha^2_{n+1}\cdot C_{n+1}}{3A_{n+1}}\right)^2\Bigg] \tag{4}$$

where

$$A_{n+1} = \left(\frac{1+\alpha_{n+1}}{1-\alpha_{n+1}}\right)^{2\alpha_{n+1}}\cdot\frac{1+\sqrt{1-(\frac{h_{mn+1}}{\lambda_g/2})^2}}{1-\sqrt{1-(\frac{h_{mn+1}}{\lambda_g/2})^2}} - \frac{1+3\alpha^2_{n+1}}{1-\alpha^2_{n+1}}$$

$$A'_{n+1} = \left(\frac{1+\alpha_{n+1}}{1-\alpha_{n+1}}\right)^{\frac{2}{\alpha_{n+1}}}\cdot\frac{1+\sqrt{1-(\frac{h_{mn}}{\lambda_g/2})^2}}{1-\sqrt{1-(\frac{h_{mn}}{\lambda_g/2})^2}}$$

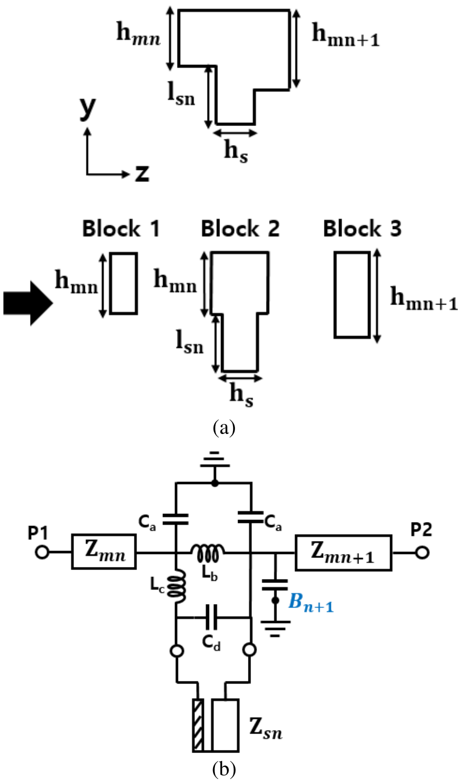

FIGURE 6. Single trough connected to a step-impedance waveguide. (a) Block diagram. (b) Equivalent circuit.

$$+\frac{3+\alpha_{n+1}^2}{1-\alpha_{n+1}^2}$$

$$C_{n+1}=\left(\frac{4\alpha_{n+1}}{1-\alpha_{n+1}^2}\right)^2$$

$$\alpha_{n+1}=\frac{h_{mn}}{h_{mn+1}}$$

The physical parameters for the step-impedance waveguide of part B with the height changing from 3.03 mm to 9.53 mm can be obtained by using the concept of the exponential tapered transmission line [40] following the design steps summarized below

1) The first step is to preset the number of troughs. Our suggestion is to initially set it to the integer close to a third or quarter of the number of troughs in part A.
2) The second step is to calculate the initial height of each section using the exponential function for a tapered transmission line [40]. Fig. 7 shows part B with 5 troughs for illustration. There are 5 changes in the height and the 6 different heights can be initially determined by using the exponential function given by

$$h(z)=h(0)e^{\frac{z}{L}\ln(\frac{h(L)}{h(0)})}(for\ 0<z<L) \tag{5}$$

where L is the length of part B and $h(0)$ and $h(L)$ are the heights of part B at its two ends which are 3.03 mm and 9.53 mm, respectively. As the heights at the two ends are fixed, the initial values of four different heights are set in this design step.

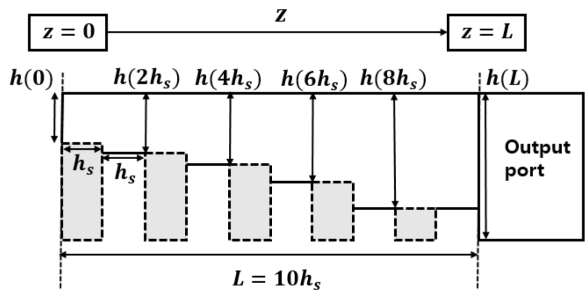

FIGURE 7. Part B between part A and the output port. (Solid line: step-impedance waveguide. Dashed line: trough)

3) The third step is to fine tune the heights, if necessary.
4) When the return loss performance needs more improvement, it is required to increase the number of troughs and repeat steps 2 and 3.

With 5 troughs in part B, calculation of the initial heights using (5) gives 3.03, 3.81, 4.79, 6.03, 7.58, and 9.53 in mm. Fig. 8 shows the circuit diagram of the entire circuit composed of parts A and B, and its frequency response is depicted by the dotted lines in Fig. 9 when parts A and B have the initial dimensions mentioned above. The return loss decreases as the frequency increases toward the cutoff frequency. Hence, as mentioned above, the initial heights have been tuned for improving the return loss. In this work, tuning has been carried out focusing on improving the return loss at the frequencies close to the cutoff frequency since the passband edge is the most sensitive to the dimension variations [41]. The heights after fine tuning are 3.03, 3.53, 4.73, 5.73, 7.33, and 9.53 in mm. The solid lines in Fig. 9 show the frequency response after fine tuning.

We have demonstrated that the rapid design of a filter with a steep skirt response can be carried out using equivalent circuits. Another advantage of using equivalent circuits instead of electromagnetic simulations is that it allows for rapid sensitivity analysis. We conducted a sensitivity analysis to observe response variations, and Fig. 10 shows the result when trough dimensions were assumed to have tolerances of up to $\pm 50\ \mu$m.

C. ENTIRE STRUCTURE

For verifying the efficient circuit-based design approach, the design parameters of parts A and B have been applied to building our waveguide filter, and Fig. 11 shows the waveguide filter structure made of parts A and B. The input and output ports are WR-75 waveguide structure as specified. The rounded-corners are formed in the filter structure considering the milling bit diameter. It can be observed that the identical troughs are cascaded by a uniform waveguide in part A. On the other hand, part B consists of the troughs with different lengths cascaded by the step-impedance waveguides. Fig. 12 shows the comparison between the circuit response and the EM simulations of the waveguide structures with and without the rounded-corners. Overall, the 3 responses agree well with one another with very

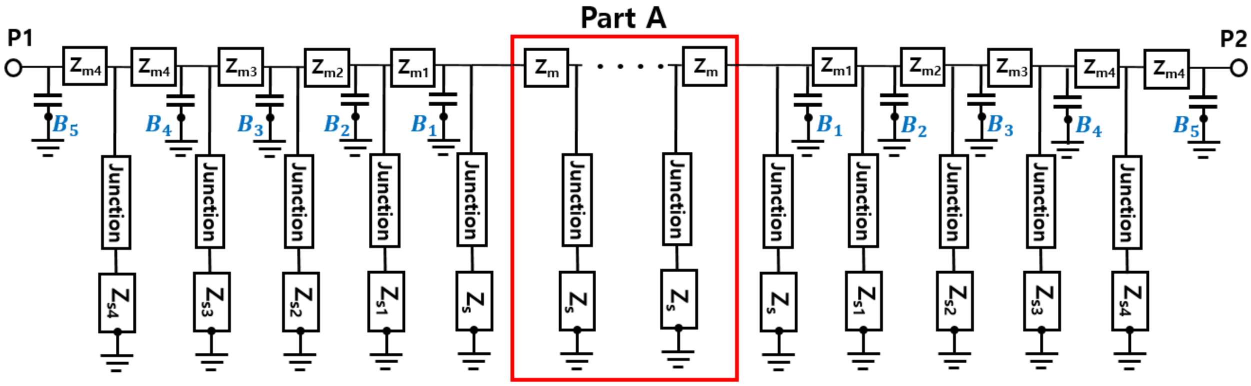

FIGURE 8. Circuit diagram of the structure composed of parts A and B.

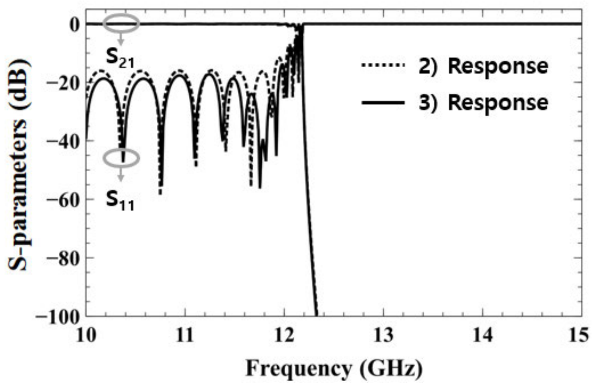

FIGURE 9. Frequency responses of the circuit diagram in Fig. 8 before (dotted lines) and after (solid lines) tuning the initial dimensions of part B.

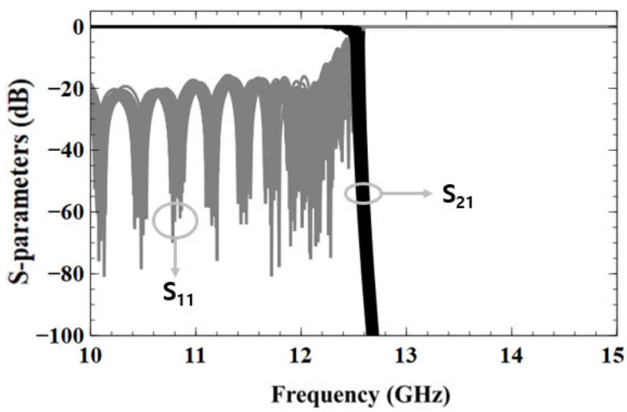

FIGURE 10. Sensitivity analysis with fabrication tolerance (±50 μm) of trough dimensions in parts A (h_m, h_s, l_s) and B (h_{mn}, l_{sn}).

small discrepancies, which indicates that it is not necessary to carry out electromagnetic simulations in determining the physical dimensions of parts A and B so far. However, our initial design does not satisfy the passband specification (10.5 - 12.5 GHz). Hence, it is required to carry out trimming the initial design such that the specifications are satisfied. This can be executed mainly by shifting the initial response to a higher frequency with rarely changing the response shape. Hence, this work proposes to shrink the width of the entire structure. In adjusting the initial dimensions, carrying out

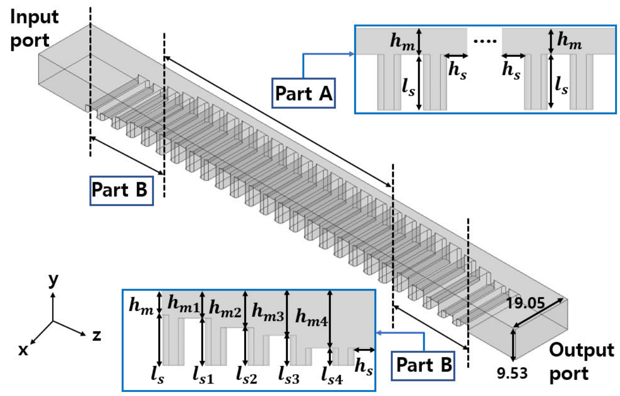

FIGURE 11. Waveguide filter structure composed of parts A and B.

electromagnetic simulations without rounded corners are not necessary since we already compared the two cases with and without rounded corners and the filter will be fabricated containing rounded corners. Our analysis accompanied by observing the frequency response with various widths has disclosed that reducing the width from 19.05 mm to 17.8 mm makes the filter have passband up to 12.5 GHz.

The dotted lines in Fig. 13 show the EM simulation of the filter structure shown in Fig. 11 when the width of parts A and B is reduced to 17.8 mm. Although the filter structure has a good return loss performance in the passband, the return loss can be further improved by addressing the change of the waveguide width between part B and the port. The impedance mismatch due to the change of the width can be mitigated by adding two troughs in the two WR-75 waveguide structures as shown in Fig. 1. The EM simulation of the structure shown in Fig. 1 is depicted by the solid lines in Fig. 13. It can be observed that the existence of the troughs in the WR-75 waveguide structures improves the return loss performance. Although the return loss near the band edge is slightly smaller than 15 dB, it is acceptable at this point since the width of parts A and B will be further reduced due to silver plating which would push the last $|S_{11}|$ lobe larger than -15 dB beyond the stop frequency of the passband (12.5 GHz). In addition, tuning screws can tune the response to some extent after fabrication. The attenuation increases by

TABLE 1. Comparison between this work and previous works.

Works	Structure	Size (Length)	Passband		Stopband		$FOM_{A\ dB}$
			Start frequency (f_1)	Stop frequency (f_2)	Start frequency with attenuation (A dB) (f_3)	Attenuation (A dB)	
[12]	Double-sided corrugated	$2.38 \cdot \lambda_g$	10.3 GHz	12.7 GHz	13.5 GHz	60 dB (measurement)	0.333
[13]	Double-sided corrugated	$0.98 \cdot \lambda_g$	10.7 GHz	13 GHz	17.2 GHz	80 dB (specification)	1.826
[14]	Double-sided corrugated	Not provided	10.7 GHz	13 GHz	13.75 GHz	80 dB (specification)	0.326
[16]	Single-sided corrugated	Not provided	17.3 GHz	22 GHz	27 GHz	50 dB (specification)	1.064
[18]	Double-sided corrugated	$7 \cdot \lambda_g$	17.7 GHz	20.2 GHz	27.5 GHz	80 dB (specification)	2.92
[22]	Single-ridged	Not provided	12.2 GHz	12.7 GHz	14 GHz	60 dB (measurement)	2.6
[23]	Double-ridged	$1.54 \cdot \lambda_g$	26 GHz	40 GHz	52 GHz	60 dB (specification)	0.857
[24]	Double-ridged	$1.52 \cdot \lambda_g$	26 GHz	40 GHz	52 GHz	70 dB (specification)	0.857
[31]	Waffle-iron	Not provided	10.7 GHz	11.7 GHz	17 GHz	60 dB (specification)	5.3
[32]	Waffle-iron	$1.14 \cdot \lambda_g$	10.7 GHz	12.5 GHz	14.5 GHz	75 dB (specification)	1.111
[33]	Quasi-periodic	$6.29 \cdot \lambda_g$	10.7 GHz	12.7 GHz	13.75 GHz	60 dB (specification)	0.525
[34]	Quasi-periodic	$7.93 \cdot \lambda_g$	10.7 GHz	12.7 GHz	13.75 GHz	60 dB (specification)	0.525
[35]	Quasi-periodic	$6.29 \cdot \lambda_g$	10.7 GHz	12.7 GHz	13.75 GHz	60 dB (specification)	0.525
[36]	Quasi-periodic	$6.8 \cdot \lambda_g$	17.5 GHz	21.5 GHz	23.5 GHz	60 dB (specification)	0.5
[38]	Meandered	$0.78 \cdot \lambda_g$	10.7 GHz	11.7 GHz	13.75 GHz	60 dB (specification)	2.05
This work (specification)	**Single-sided corrugated**	$\mathbf{4.66 \cdot \lambda_g}$	**10.5 GHz**	**12.5 GHz**	**12.75 GHz**	**90 dB**	**0.125**
This work (measurement)			**10 GHz**	**12.525 GHz**	**12.67 GHz**	**60 dB**	**0.057**
					12.69 GHz	**70 dB**	**0.065**
					12.71 GHz	**80 dB**	**0.073**
					12.73 GHz	**90 dB**	**0.081**
					12.74 GHz	**95 dB**	**0.085**

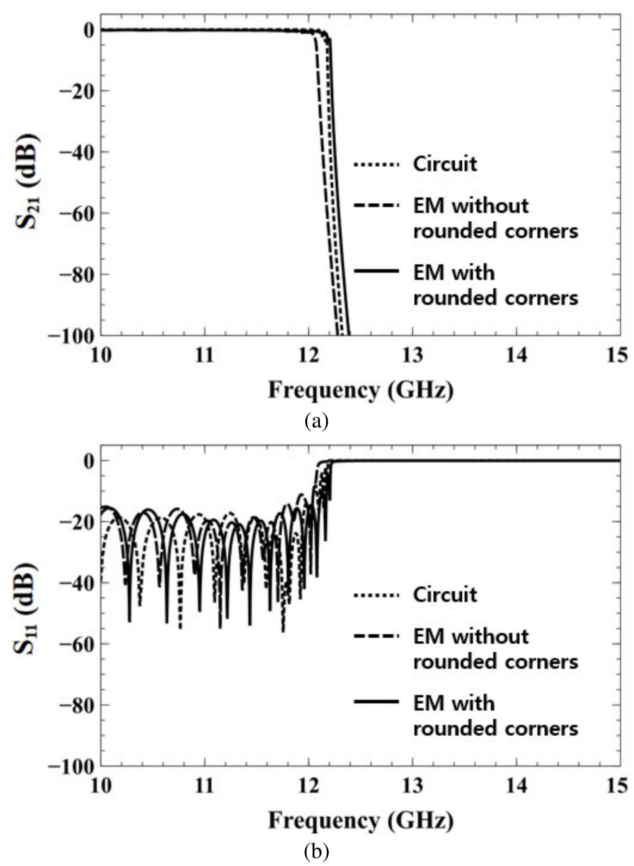

FIGURE 12. The frequency responses of the circuit schematic (dotted lines) and electromagnetic simulations of the filter structure shown in Fig. 11 with (solid lines) and without (dashed lines) rounded corners. (a) Transmission response. (b) Reflection response.

100 dB from 12.5 GHz to 12.75 GHz, which indicates that the filter produces a very steep skirt response satisfying our target specification.

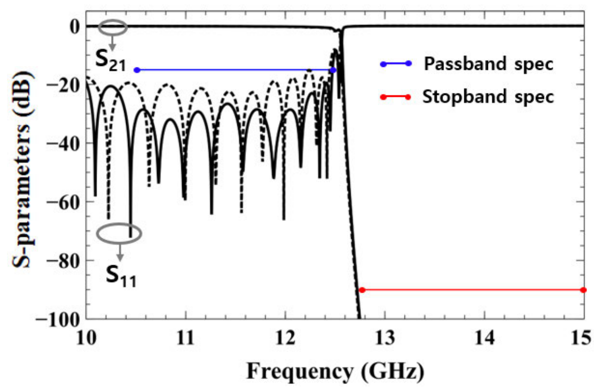

FIGURE 13. Dotted lines: EM simulation of the structure shown in Fig. 11 when the width of parts A and B is reduced to 17.8 mm. Solid lines: EM simulation of the structure shown in Fig. 1.

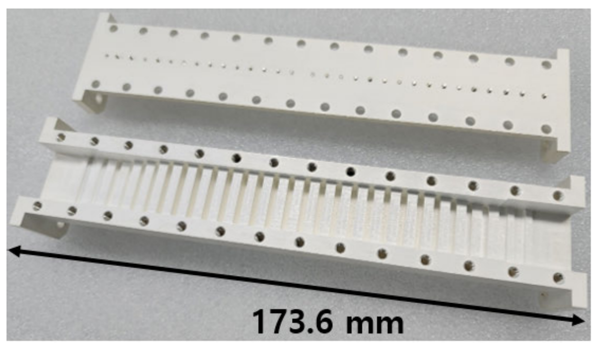

FIGURE 14. Fabricated filter with the cover unassembled.

III. FABRICATION AND MEASUREMENT

For verification, the filter structure in Fig. 1 has been fabricated and measured. Fig. 14 shows the fabricated filter with the cover unassembled. The cover contains tuning screws to have fabrication tolerance. It is made with aluminum and the structure has been fabricated by milling, drilling and silver plating. In Fig. 15, the measured response

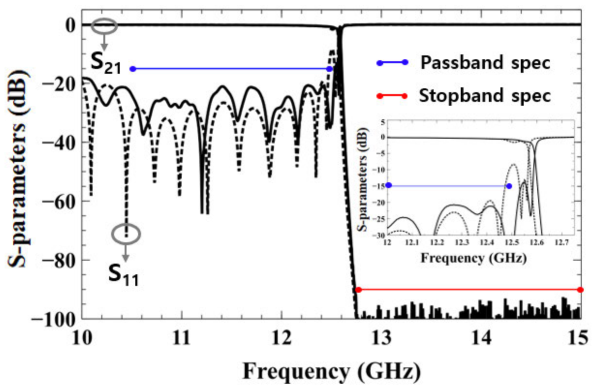

FIGURE 15. **Comparison between the measurement (solid lines) and the electromagnetic simulation (dotted lines).**

is compared to the electromagnetic simulation. It can be seen that the filter produces a wide passband with the return loss larger than 20 dB in the passband from 10.5 to 12.5 GHz. The stopband attenuation is larger than 90 dB with a very steep skirt response in the transition band. The measured result of the fabricated filter validates our practical circuit-based design approach for a waveguide lowpass filter with a steep skirt response.

Table 1 shows the comparison between this work and previous works on waveguide lowpass filters. As mentioned earlier, a filter with a smaller FOM has a steeper skirt response. Our filter is required to have a $FOM_{90\ dB}$ of 0.125. This indicates that the attenuation needs to increase by 90 dB within the transition band whose width is 0.125 times the passband width. Table 1 also provides the measured $FOM_{A\ dB}$ with various attenuation values to facilitate easy comparisons with previous works. It can be concluded that our filter has a steeper skirt response than filters reported in the literature.

IV. CONCLUSION

This work has presented a practical circuit-based design approach for a waveguide lowpass filter with a high attenuation performance in the stopband close to the passband. By virtue of the proposed design approach based on circuit analysis, the design can be carried out without heavily relying on electromagnetic simulations. Our design approach enabled us to rapidly achieve an extremely steep skirt response, whereas conventional design approaches relying on electromagnetic simulations often require a tremendous amount of time making an entire filter design procedure highly exhaustive. The proposed design approach has been demonstrated using a WR-75 filter example required to have an extremely steep skirt response. The design approach can be applied to waveguide lowpass filters operating in different frequency bands.

REFERENCES

[1] M. Hayati, A. Rezaei, and L. Noori, "Design of a high–performance lowpass–bandpass diplexer using a novel microstrip structure for GSM and WiMAX applications," *IET Circuits, Devices Syst.*, vol. 13, no. 3, pp. 361–367, May 2019.

[2] G. Moloudian, S. Bahrami, and R. M. Hashmi, "A microstrip lowpass filter with wide tuning range and sharp roll-off response," *IEEE Trans. Circuits Syst. II, Exp. Briefs*, vol. 67, no. 12, pp. 2953–2957, Dec. 2020.

[3] N. Stojanovic, N. Stamenkovic, and I. Krstic, "Design of modified Jacobi microstrip lowpass filter for L-band application," *IEEE Trans. Circuits Syst. II, Exp. Briefs*, vol. 69, no. 12, pp. 5154–5158, Dec. 2022.

[4] Y. Zeng, M. Yu, and Z. P. Tan, "Novel compact lowpass filter using dual-layer coupled resonators," *IEEE Trans. Microw. Theory Techn.*, vol. 71, no. 9, pp. 3937–3944, Sep. 2023.

[5] M. Hayati, R. Salahi, M. Akbari, S. Zargari, and D. Abbott, "Low complexity compact lowpass filter using T-shaped resonator loaded with a stub," *IEEE Access*, vol. 11, pp. 35763–35769, 2023.

[6] S. B. Cohn, "Analysis of a wide-band waveguide filter," *Proc. IRE*, vol. 37, no. 6, pp. 651–656, Jun. 1949.

[7] S. B. Cohn, "Design relations for the wide-band waveguide filter," *Proc. IRE*, vol. 38, no. 7, pp. 799–803, Jul. 1950.

[8] R. Levy, "Tapered corrugated waveguide low-pass filters," *IEEE Trans. Microw. Theory Techn.*, vol. MTT-21, no. 8, pp. 526–532, Aug. 1973.

[9] W. Hauth, R. Keller, and U. Rosenberg, "CAD of waveguide low-pass filters for satellite applications," in *Proc. 17th Eur. Microw. Conf.*, Rome, Italy, Oct. 1987, pp. 151–156.

[10] O. Monerris, P. Soto, S. Cogollos, V. E. Boria, J. Gil, C. Vicente, and B. Gimeno, "Accurate circuit synthesis of low-pass corrugated waveguide filters," in *Proc. Eur. Microw. Conf.*, Sep. 2010, pp. 1237–1240.

[11] F. De Paolis, R. Goulouev, J. Zheng, and M. Yu, "CAD procedure for high-performance composite corrugated filters," *IEEE Trans. Microw. Theory Techn.*, vol. 61, no. 9, pp. 3216–3224, Sep. 2013.

[12] F. Teberio, I. Arregui, A. Gomez-Torrent, E. Menargues, I. Arnedo, M. Chudzik, M. Zedler, F. J. Görtz, R. Jost, T. Lopetegi, and M. A. G. Laso, "Low-loss compact Ku-band waveguide low-pass filter," in *IEEE MTT-S Int. Microw. Symp. Dig.*, Phoenix, AZ, USA, May 2015, pp. 1–4.

[13] F. Teberio, I. Arregui, M. Guglielmi, A. Gomez-Torrent, P. Soto, M. A. G. Laso, and V. E. Boria, "Compact broadband waveguide diplexer for satellite applications," in *IEEE MTT-S Int. Microw. Symp. Dig.*, San Francisco, CA, USA, May 2016, pp. 1–4.

[14] F. Teberio, I. Arregui, P. Soto, M. A. G. Laso, V. E. Boria, and M. Guglielmi, "High-performance compact diplexers for Ku/K-band satellite applications," *IEEE Trans. Microw. Theory Techn.*, vol. 65, no. 10, pp. 3866–3876, Oct. 2017.

[15] F. Teberio, I. Arnedo, J. M. Percaz, I. Arregui, T. Lopetegi, and M. A. G. Laso, "Accurate design of corrugated waveguide low-pass filters using exclusively closed-form expressions," in *Proc. Eur. Microw. Conf.*, Nuremberg, Germany, Oct. 2017, pp. 632–635.

[16] D. Smacchia, C. Carceller, M. Guglielmi, P. Soto, V. Boria, J. Ruiz, and P. González, "A wideband diplexer for Ka-band passive intermodulation measurement," in *IEEE MTT-S Int. Microw. Symp. Dig.*, Philadelphia, PA, USA, Jun. 2018, pp. 1106–1109.

[17] M. Cetin, G. Boyacioglu, B. Alicioglu, and N. Yildirim, "Synthesis approach for compact Ku-band waveguide lowpass filters with wide rejection bandwidth," in *Proc. 18th Medit. Microw. Symp. (MMS)*, Istanbul, Turkey, Oct. 2018, pp. 221–224.

[18] S. Sirci, E. Menargues, and M. Billod, "Space-qualified additive manufacturing and its application to active antenna harmonic filters," in *IEEE MTT-S Int. Microw. Symp. Dig.*, Perugia, Italy, Nov. 2021, pp. 239–242.

[19] S. B. Cohn, "Properties of ridge wave guide," *Proc. IRE*, vol. 35, no. 8, pp. 783–788, Aug. 1947.

[20] S. Hopfer, "The design of ridged waveguides," *IEEE Trans. Microw. Theory Techn.*, vol. MTT-3, no. 5, pp. 20–29, Oct. 1955.

[21] D. Dasgupta and P. K. Saha, "Rectangular waveguide with two double ridges," *IEEE Trans. Microw. Theory Techn.*, vol. MTT-31, no. 11, pp. 938–941, Nov. 1983.

[22] A. M. K. Saad, "Novel lowpass harmonic filters for satellite application," in *IEEE MTT-S Int. Microw. Symp. Dig.*, San Francisco, CA, USA, 1984, pp. 292–294.

[23] A. Kirilenko, L. Rud', and V. Tkachenko, "Harmonic filters on ridged waveguides," in *Proc. Int. Kharkov Symp. 'Physics Eng. Millim. Submillimeter Waves'*, vol. 1, Kharkov, Ukraine, Sep. 1998, pp. 323–325.

[24] A. Kirilenko, L. Rud', V. Tkachenko, and D. Kulik, "Design of bandpass and lowpass evanescent-mode filters on ridged waveguides," in *Proc. 29th Eur. Microw. Conf.*, Munich, Germany, Oct. 1999, pp. 239–242.

[25] S. Li, J. Fu, and X. Wu, "Double ridged waveguide low pass filters for satellite application," in *Proc. Int. Symp. Microw. Antenna Propag. (EMC)*, Hangzhou, China, Aug. 2007, pp. 408–410.
[26] E. D. Sharp, "A high-power wide-band waffle-iron filter," *IEEE Trans. Microw. Theory Techn.*, vol. MTT-11, no. 2, pp. 111–116, Mar. 1963.
[27] L. Young and B. M. Schiffman, "New and improved types of waffle-iron filters," *Proc. Inst. Electr. Eng.*, vol. 110, no. 7, pp. 1191–1198, 1963.
[28] F. Arndt, R. Beyer, W. Hauth, D. Schmitt, and H. Zeh, "Cascaded wide stop band waffle-iron filter designed with a MM/FE CAD method," in *Proc. 29th Eur. Microw. Conf.*, Munich, Germany, Oct. 1999, pp. 186–189.
[29] F. Arndt and J. Brandt, "Direct EM based optimization of advanced waffle-iron and rectangular combline filters," in *IEEE MTT-S Int. Microw. Symp. Dig.*, vol. 3, Seattle, WA, USA, Jun. 2002, pp. 2053–2056.
[30] M. B. Manuilov and K. V. Kobrin, "Field theory CAD of waffle-iron filters," in *Proc. Eur. Microw. Conf.*, Paris, France, 2005, p. 1230.
[31] F. Teberio, I. Arnedo, J. M. Percaz, I. Arrcgui, P. Martin-Iglesias, T. Lopetcgi, and M. A. G. Laso, "Accurate design procedure for waffle-iron low-pass filter," in *IEEE MTT-S Int. Microw. Symp. Dig.*, Philadelphia, PA, USA, Jun. 2018, pp. 1238–1241.
[32] F. Teberio, J. M. Percaz, I. Arregui, P. Martin-Iglesias, T. Lopetegi, M. A. G. Laso, and I. Arnedo, "Design procedure for new compact waffle-iron filters with transmission zeros," *IEEE Trans. Microw. Theory Techn.*, vol. 66, no. 12, pp. 5614–5624, Dec. 2018.
[33] I. Arregui, I. Arnedo, A. Lujambio, M. Chudzik, D. Benito, R. Jost, F.-J. Gortz, T. Lopetegi, and M. A. G. Laso, "A compact design of high-power spurious-free low-pass waveguide filter," *IEEE Microw. Wireless Compon. Lett.*, vol. 20, no. 11, pp. 595–597, Nov. 2010.
[34] I. Arregui, F. Teberio, I. Arnedo, A. Lujambio, M. Chudzik, D. Benito, R. Jost, F. J. Gortz, T. Lopetegi, and M. A. G. Laso, "High-power low-pass harmonic waveguide filter with TE_{n0}-mode suppression," *IEEE Microw. Wireless Compon. Lett.*, vol. 22, no. 7, pp. 339–341, Jul. 2012.
[35] I. Arregui, F. Teberio, I. Arnedo, A. Lujambio, M. Chudzik, D. Benito, T. Lopetegi, R. Jost, F.-J. Görtz, J. Gil, C. Vicente, B. Gimeno, V. E. Boria, D. Raboso, and M. A. G. Laso, "Multipactor-resistant low-pass harmonic filters with wide-band higher-order mode suppression," in *IEEE MTT-S Int. Microw. Symp. Dig.*, Seattle, WA, USA, Jun. 2013, pp. 1–4.
[36] F. Teberio, I. Arregui, A. Gomez-Torrent, E. Menargues, I. Arnedo, M. Chudzik, M. Zedler, F.-J. Görtz, R. Jost, T. Lopetegi, and M. A. G. Laso, "High-power waveguide low-pass filter with all-higher-order mode suppression over a wide-band for Ka-band satellite applications," *IEEE Microw. Wireless Compon. Lett.*, vol. 25, no. 8, pp. 511–513, Aug. 2015.
[37] P. V. Castejón, D. C. Serrano, F. D. Q. Pereira, J. Hinojosa, and A. Álvarez Melcón, "A novel low-pass filter based on rounded posts designed by an alternative full-wave analysis technique," *IEEE Trans. Microw. Theory Techn.*, vol. 62, no. 10, pp. 2300–2307, Oct. 2014.
[38] F. Teberio, J. M. Percaz, I. Arregui, P. Martin-Iglesias, T. Lopetegi, M. A. G. Laso, and I. Arnedo, "Rectangular waveguide filters with meandered topology," *IEEE Trans. Microw. Theory Techn.*, vol. 66, no. 8, pp. 3632–3643, Aug. 2018.
[39] N. Marcuvitz, *Waveguide Handbook*. New York, NY, USA: McGraw-Hill, 1951.
[40] D. M. Pozar, *Microwave Engineering*. New York, NY, USA: Wiley, 2005, ch. 5, pp. 262–263.
[41] A. B. Jayyousi, M. J. Lancaster, and F. Huang, "Filtering functions with reduced fabrication sensitivity," *IEEE Microw. Wireless Compon. Lett.*, vol. 15, no. 5, pp. 360–362, May 2005.

SANGGU LEE was born in Seoul, South Korea, in 1993. He received the B.E. degree in electronic engineering from Ajou University, Suwon, South Korea, in 2018, and the Ph.D. degree in radio communications engineering from Korea University, Seoul, in 2023.

In 2023, he joined LIGNex1, Leading Innovation Group, where he is involved in multibeam antenna for national defense. His current research interests include RF front-end modules and AESA antenna systems.

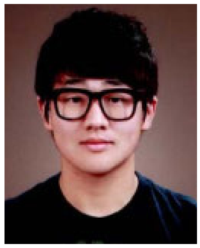

JONGHEUN LEE (Graduate Student Member, IEEE) received the B.E. degree in computer and communication engineering from Korea University, Seoul, South Korea, in 2019, where he is currently pursuing the Ph.D. degree in radio communications engineering.

His current research interest includes planar microwave circuits. He was a recipient of the First Prize in the Student and Young Engineer Design Competition of 2022 Asia–Pacific Microwave Conference.

DUCKKI BAEK was born in Yeongju-si, South Korea. He received the B.E. degree from Namseoul University, in 2002.

He was a Chief Researcher with Telwave, from 1995 to 2005, M&M Lynx, from 2006 to 2011, and Qnion, from 2011 to 2016. He has been running PILAS Company Ltd., since 2016. The main concerns are developing the RF components in the defense and satellite industries.

PILYONG LEE was born in Asan-si, South Korea. He received the M.E. degree from Soonchunhyang University, in 2000.

He was a Chief Researcher with Telwave, from 2000 to 2005, M&M Lynx, from 2006 to 2011, and Qnion, from 2011 to 2013. He has been running PILAS Company Ltd., since 2015. The main concerns are developing the RF modules in the defense and satellite industries.

JUSEOP LEE (Senior Member, IEEE) received the B.Eng. and M.Eng. degrees in radio science and engineering from Korea University, Seoul, South Korea, in 1997 and 1999, respectively, and the Ph.D. degree in electrical engineering from the University of Michigan, Ann Arbor, MI, USA, in 2009.

He joined the Electronics and Telecommunications Research Institute (ETRI), Daejeon, South Korea, in 2001, where he was involved in the design of passive microwave equipment for Ku- and Ka-band communications satellites. In 2005, he joined the University of Michigan, where he was a Research Assistant and a Graduate Student Instructor with the Radiation Laboratory and he was involved in research activities focused on millimeter-wave radars and synthesis techniques for multiple-passband microwave filters. In 2009, he joined Purdue University, West Lafayette, IN, USA, as a Postdoctoral Research Associate, where he was involved in the design of adaptable RF systems. In 2012, he joined Korea University, where he is currently a Professor. From 2019 to 2020, he was a Visiting Professor with the University of Virginia, Charlottesville, VA, USA. His current research interests include RF and microwave circuits, satellite transponders, and wireless power transfer systems.

Prof. Lee was a recipient of the Best Teaching Award presented by Korea University for Spring 2018 and Fall 2018. He was an Associate Editor of IEEE Transactions on Microwave Theory and Techniques, from 2017 to 2019.